

The HYPespectral Stereo Observing System

G. Cremonese¹, G. Naletto^{2,1}, C. Re¹, M. Tordi³, I. Dorgnach⁴, C. Doria⁴, R. La Grassa¹, A. Meneguzzo⁴, L. Agostini⁵, F. Brotto², M. Faccioni², L. Lessio¹, C. Bettanini⁴, F. Capaccioni⁵, E. Giovine⁶, F. Lazzarotto¹, L. Marinangeli⁷, F. Mattioli⁶

¹ National Institute of Astrophysics – Astronomical Observatory of Padova, vicolo Osservatorio 5, Padova, 35122, Italy

² University of Padova, Department of Physics and Astronomy, Via F. Marzolo 8, 35131, Padova, Italy

³ EIE GROUP Srl, Via Torino 151/A, 30172 Mestre VE, Italy

⁴ Center of Studies and Activities for Space CISAS “G. Colombo”, University of Padova, Via Venezia 1, 35131 PD, Italy

⁵ Institute for Space Astrophysics and Planetology, INAF, Tor Vergata Via del Fosso del Cavaliere, 100 - 00133 Roma, Italy, e-mail: gabriele.cremonese@inaf.it

Remaining affiliations can be found at the end of the paper.

Abstract. The HYPerspectral Stereo Observing System (HYPSOS) is a novel remote sensing pushbroom instrument able to give simultaneously both 3D spatial and spectral information of the observed features. HYPSOS is a very compact instrument, which makes it attractive for both possible planetary observation and for its use on a nanosat, e.g. for civilian applications. This instrument collects light from two different perspectives, as a classical pushbroom stereocamera, which allows one to achieve the three-dimensional model of the observed surface, and then to extract the spectral information from each resolved element, thus obtaining a full 4-dimensional hypercube dataset. To demonstrate the actual performance of this novel type of instrument, we realized a HYPSOS prototype, that is an instrument breadboard to be tested in a laboratory environment. For checking its performance, we setup an optical facility representative of a possible flight configuration. In this paper we provide a description of HYPSOS concept, of its opto-mechanical design and of the ground support equipment used to characterize the instrument. Some preliminary results are described.

Key words. Instrument: stereo camera

1. Introduction

Remote sensing observations often require to couple the information acquired by an imaging system with the one acquired by a spectroscopic instrument: “patching” the spectral

characteristics of an observed region to the corresponding imaging features provides a much larger and more complete set of information than the single instruments themselves. It is quite common to find both these types of instruments on board a spacecraft, in particular

for Solar System bodies exploration, depending from the capability of the instruments and spacecraft to compress and to downlink the data. Often, to get still more information, the on-board imaging system has stereoscopic capabilities, that it provides data with which it is possible to reconstruct a digital terrain model (DTM) of the observed features. Stereo capabilities are now more and more common on remote sensing satellites, even if the data reduction is much more complicated than simple imaging: in fact, to realize a DTM it is necessary to acquire at least a couple of images of the same region from different perspectives, and all the geometrical acquisition parameters (i.e. satellite attitude and position with respect to a common reference system) have to be known with great accuracy.

The datasets acquired by merging the products of a spectrometer and a stereo camera have 4-dimensions, three spatial and one spectral, and they provide an essentially complete information about the observed regions, at least for the large majority of scientific cases of interest. Unfortunately, the possibility of obtaining homogeneous datasets is often limited by the different characteristics of the involved instruments, in terms of sensitivity, of spatial resolution on ground, field of view (FoV), coordinated observations, overlapping spectral ranges, and so on. To solve this issue, a very accurate instrument cross-calibration would be needed, that it might be difficult to obtain, mainly if the instruments are realized by different teams with different on ground support equipment and different calibration procedures.

For example, the current approach used for Mars' investigation consists in reconstructing the 3D mineralogical stratigraphy (Grotzinger et al. (2012)) combining detailed topography overlapped with colour-coded images representing the compositional variations. Stratigraphy is a fundamental information because it records multiple Mars environments in sequential age order and allows the reconstruction of the past geological and climatic history of the planet. However, the heterogeneous spatial and spectral resolutions of available martian datasets allow to perform this type of anal-

ysis in very limited locations. Thus, it is crucial to have a dataset such as the one produced by HYPPOS to correctly decipher the past evolution of Mars.

To our knowledge, these problems exist with all remote sensing satellites, also those which have full attitude control and are presently used for Earth Observation.

To overcome this problem, we thought about the possibility of developing an instrument which has simultaneously both stereoscopic and spectroscopic capabilities, in practice an instrument able to provide a spectral DTM of the observed region as a final product. Such an instrument, clearly more complicated than either a stereoscopic imaging system or a spectroscopic one, would intrinsically solve all the problems related to instrument cross-calibration, being a single instrument summarizing all the capabilities of the merged two: it would be sufficient to properly calibrate this instrument to be able to fully characterize the observed spectral and spatial surface features in an optimal way.

If this is feasible, a single instrument would provide practically all the information needed to fully characterize a planet surface element, without the need to merge the data provided by different instruments. When designing this instrument, we had in mind a system configuration with a nadir pointing satellite and a pushbroom stereo camera (with a forward and a backward channels, tilted at $\pm\Theta$ with respect to nadir along the flying direction) specific for a planetary observation, and the emphasis was mainly on the scientific return of the observations; however, definitely the same approach can be adapted to realize low-cost Earth 4D-observing systems, like nanosats or Unmanned Aerial Vehicles (UAVs), mainly for civilian applications, for example in agriculture or geology. In such a case the system optical configuration will have to be optimized for the specific application, but this is a minor issue as the validity of this novel concept is confirmed.

2. HYPPOS Optical design

HYPPOS represents a novel remote sensing pushbroom instrument which combines the

3D information of a classical stereo camera with the spectral sampling, thus providing a simultaneous 4D information, spatial and spectral, of the observed features. One of the main drivers of the HYPPOS project was to design a compact instrument, compatible with small satellite applications, ranging from planetary exploration to terrestrial environmental monitoring. We started from the experience we gained on SIMBIO-SYS Cremonese et al. (2020), that is the suite of three remote sensing instruments on board the BepiColombo mission sharing the Main Electronics and under the responsibility of one team, and in particular on the stereo camera STC. SIMBIO-SYS will improve the scientific return on observing the Mercury surface taking advantage of the common operations, planning and reduction, and making the data fusion a normal activity of any member of the team. But this instrument suite is based on 3 different optical designs, each having different calibrations and resolutions.

The outcome of our new idea is an instrument in which the two optical paths, needed for getting the 3D information, merge along a single optical train and then pass through the entrance slit of an imaging spectrometer which disperses the spectrum on a single 2D detector.

STC is a very compact camera system, in which light is collected from two fixed channels tilted by 20° with respect to nadir, sent to a common optical path, and finally collected by a single bidimensional sensor Da Deppo et al. (2010). To minimize mass and envelope, we designed the HYPPOS telescope with a concept similar to the STC one, collecting the light from two independent channels and sending them along a common optical path. There are however differences with respect to STC: first, the telescope configuration is no longer based on a modified Schmidt camera as in STC, but on a three mirror anastigmatic (TMA) configuration; then, on the telescope focal plane there is not the focal plane assembly, but the entrance slit of the HYPPOS spectrometer; in addition, to have a single entrance slit spectrometer, we added two 90° field rotators in front of the HYPPOS apertures.

Figure 1 shows a schematic view of the ground projected FoVs for a standard two-cameras pushbroom stereo system with a nadir pointing satellite: in addition to Channel 1 (forward) and Channel 2 (backward) FoVs, we can see the spacecraft orbit ground projection and motion orientation.

If using standard camera systems, in the hypothesis of a common focal plane, these two FoVs would be imaged as shown in Figure 2 left and such a configuration would make the production of the spectrometer much more complex, that in this case would need to have two separate entrances. Thus, by adding two field rotators, in our case two 45° tilted Schmidt-Pechan prisms, one per channel, we could rotate by 90° the FoVs obtaining on the telescope focal plane a projected image as shown in Figure 2 right. The rotation allows one to project on a single spectrometer entrance slit, which has also the function of field stop, both the channel FoVs. In addition, by suitably selecting the two FoVs, they enter the spectrometer in different portions of the entrance slit: so, thanks to the stigmatic properties of the spectrometer, the spectra of the two FoVs will be obtained independently and without any crosstalk. The choice of a different optical design for HYPPOS with respect to STC is also due to the possibility of making HYPPOS a rather versatile instrument. In fact, STC is operative in a limited portion of the visible spectrum, while HYPPOS can be extended to larger portion of the spectrum, potentially from ultraviolet to mid infrared, as a function of the scientific targets under investigation.

To verify the goodness and the quality of the just described concept, we realized an instrument prototype thanks to a grant by Italian Space Agency (ASI). On the basis of the available resources, we designed a HYPPOS prototype working in the visible portion of the spectrum, from 400 nm to 800 nm, that is enough to validate the concept of the instrument, but for future space applications the extension to the IR has high priority. Figure 3 shows the schematic of the optical design of HYPPOS pointing at all the optical elements. The telescope, after the Schmidt-Pechan

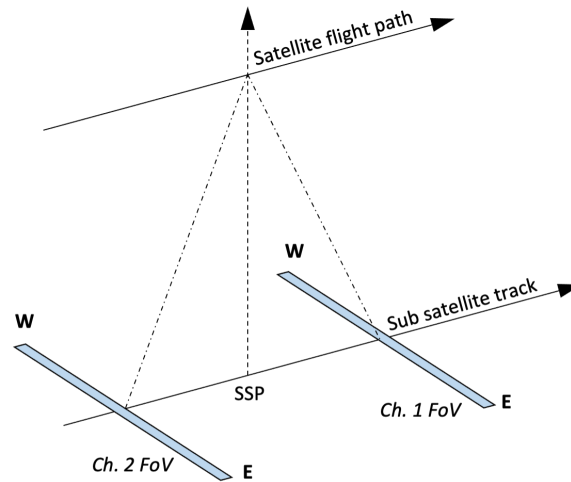


Fig. 1. Ground projection of a pushbroom stereo camera FoVs (SSP: Sub Satellite Point).

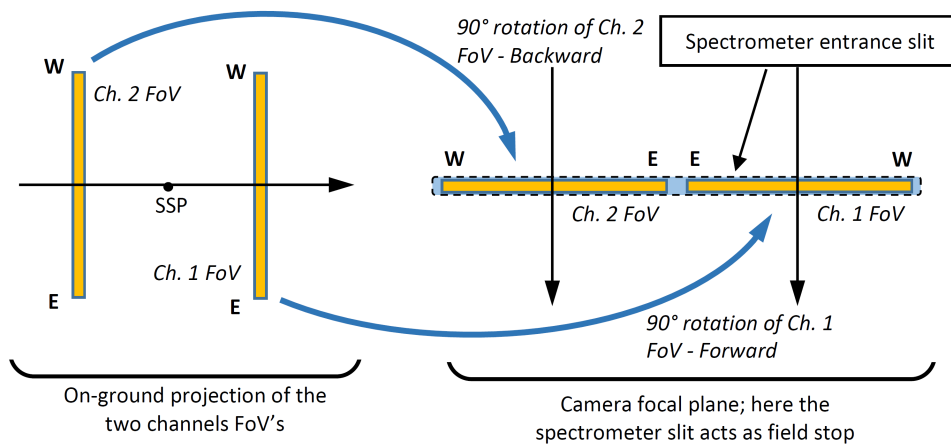


Fig. 2. On the left, the on ground projection of the HYPPOS camera system FoVs are shown; on the right, the same FoVs are shown on the camera focal plane, together with the HYPPOS spectrometer entrance slit.

prisms (SPP) is composed by the three mirrors M1, M2, M3 and the folding mirror FM. The latter could actually be replaced by a diopter, to have also a transmitted beam in addition to the reflected one: in this way, by adding a second spectrometer, the operational spectral range of HYPPOS could be extended in an

additional portion of the spectrum.

As shown in Figure 3, light entering the two channels is folded by 20° with respect to nadir by two entrance flat mirrors (EFM). The aperture stops of HYPPOS, two 35 mm diameter circular masks, one per channel, are located at the input SPP face's. Light is 90° ro-

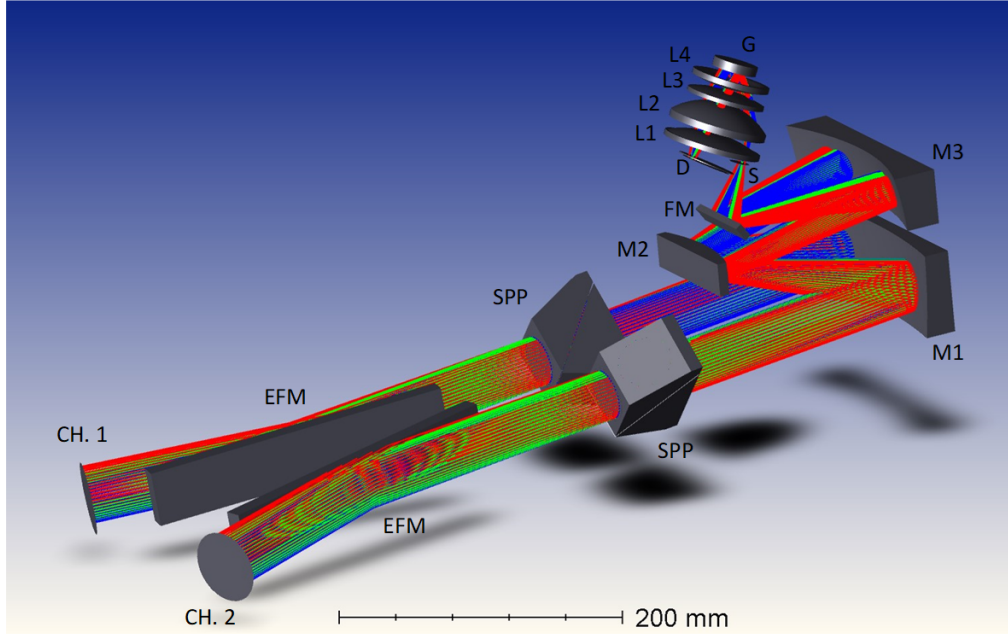


Fig. 3. Optical layout of HYPPOS. For the acronym description, see the text.

tated by SPP and illuminates two sub-apertures of the TMA mirrors; in order to limit possible stray light, suitable masks are set in front of the telescope mirrors. As mentioned before, the FoV is limited by the spectrometer entrance slit (S) on the telescope focal plane. The “slit” is actually a double-long-slit, $22\ \mu\text{m}$ wide and 8 mm long each channel, with a 1 mm obscuration in between (see Figure 2 right); given the telescope focal length of 245 mm, the nominal instantaneous FoV of HYPPOS is $18.5\ \text{arcsec} \times 1.87^\circ$; because of the folding of the two EFM, the actual across track FoV is $(20.125 - 22)^\circ$ with respect to nadir, respectively, for the two channels. More details about the HYPPOS telescope optical configuration can be found in Tordi et al. (2020) and Naletto et al. (2023); here ourselves to saying that the nominal RMS spot size at the telescope focus is well below $10\ \mu\text{m}$ over all the useful FoV. Light passing through the slit enters a double-pass imaging spectrometer, composed by four lenses (L1, L2, L3, L4) and a concave reflection grating (G). Finally, the two separate spectra are collected by a bidimensional

detector (D). The spectrometer practically has a 1:1 magnification. The nominal plate scale factor on the spectrometer focal plane is $34.7\ \text{nm/mm}$: assuming a $22\ \mu\text{m}$ sampling, we conservatively obtain a resolving spectral element (double sampling) of 1.53 nm.

3. HYPPOS prototype realization

The main aim of the experiment is to realize the prototype of HYPPOS not having strict requirements about mass and envelope, this means it has been adopted a rather solid mechanical structure holding all the optical elements, and allowing all the degrees of freedom needed to perform a proper system alignment (for this, a specific tolerance analysis of the optical design has also been done). A schematic view of the HYPPOS mechanical structure is shown in Figure 4.

The left panel of Figure 4 shows also the optical path for the central ray: after crossing the SPP on the left, the light beam is reflected by M1, M2, M3, and FM before entering a cylinder which hosts all the spectrometer

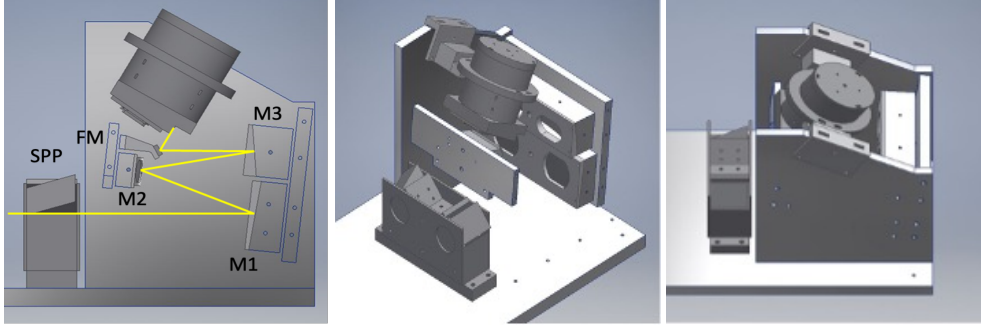


Fig. 4. The left panel shows a section view of the HYPPOS structure with the central ray optical path. In the middle an open view of the whole structure and in the right panel the complete view of HYPPOS prototype.

elements. The middle panel shows the SPP's holder which includes the instrument aperture stops. Also the mirrors have a mask in front: these masks have the function of limiting the beam aperture and to minimize the possible stray light. In this respect, it is important to bear in mind the possible cross-talk between the two channels, i.e. light from one channel outside the nominal FoV entering the other. To limit this, a baffle should be considered in front of the instrument aperture, as well a vane in between the two optical paths in proximity of the spectrometer entrance slit. Since this is not an issue with this prototype, as will be explained in the next section, we did not implement them; however, some care has to be taken when designing an actual flight instrument in order to avoid this type of problem. Finally, the right panel shows a view of the complete instrument: the cylinder, visible on the instrument top, holds all the optical elements of the spectrometer, from the entrance slit to the lenses, to the grating and the detector.

4. Laboratory setup

To reproduce in the laboratory the acquisition mode of HYPPOS we modified the facility used to calibrate STC (Simioni et al. (2017); Naletto et al. (2012)) and introduced some fore-optics to HYPPOS.

The basic idea is to send on one of the two HYPPOS apertures a FoV representative of a

planet surface, scanning it as if the instrument was flying on a satellite, then to second aperture. Having the preliminary knowledge, by suitable calibration, of the 3D profile of the surface and of its spectral characteristics, it will be possible to compare the final HYPPOS hyperspectral-DTM (HDTM) product to verify the goodness of the obtained results.

As observational target of HYPPOS we use a relatively flat stone with spectral variegations (among the others, we can use an anorthosite sample already used for calibrating STC) that can be illuminated by a halogen lamp at different incidence angles to reproduce different Sun illumination conditions. To reproduce in laboratory the pushbroom target scanning, the target and the illumination system have been mounted on a linear stage, which moves the stone surface over the HYPPOS object plane. To provide the condition of a target at very large distance from the instrument aperture, the target surface is positioned on the focal plane of a fixed collimating lens, with 1 m focal length: the light diffused by the target and collected by the lens then enters the HYPPOS apertures practically as a source at infinity. Since the same surface has to be acquired by HYPPOS from two different perspectives, i.e. the incidence angle of the central ray of the two channels are tilted by 20° , the whole system is on top of a rotating stage, that can tilt the target with the right orientation with respect to the HYPPOS acquisition perspective.

To optimize the setup on the optical bench,

it has been more convenient to replace the two folding grazing incidence mirrors before the SPP's by two couples of smaller folding mirrors at 55° and 45° incidence angles. Thanks to this fore-optics system, and mounting HYPPOS on a second rotating stage, it is possible to reproduce the acquisition from either the forward or the backward channels by a simple rotation of the whole instrument. The acquisition modes through the two HYPPOS channels, forward and backward, is shown in Figure 5: it is evident that the acquisition geometry is the same in the two cases. The practical difference is that in laboratory we move the target relative to a fixed instrument, while in-flight the instrument is moving with respect to a fixed target.

Tilt and relative position of all mirrors of the TMA prototype are adjustable by means of dedicated mounting tools. The telescope has been aligned first, without the spectrometer, by means of a dedicated illumination system, which provided two co-aligned entrance beams on the two telescope apertures, and an auxiliary camera mounted on the telescope nominal focus position. The optical performance of the TMA showed to be nominal, even if the slightly undersized illumination system provided a diffraction limited setup. Concerning the optically less critical spectrometer, all the lenses have been mounted in their nominal position by simple mechanical tolerance; the grating is instead mounted on a dedicated holder fixed to the top cylinder closing flange by a system which allows its alignment. Internally, we also included a zero order light trap to minimize the stray light inside the cylinder. Finally, the detector is attached to the bottom cylinder flange; the latter also supports the spectrometer entrance slit.

HYPPOS mechanical structure has been realized in our internal workshop, with the exception of few pieces done by a local company by means of 3D additive manufacturing. All the optical elements have been realized by local Italian companies, with the exception of the grating which is off-the-shelf. The spectrometer entrance slit has been realized by means of nanotechnologies, as already done for the ELENA shutter on board of

BepiColombo (Mattioli et al. (2011); Rispoli et al. (2013)): first a mask is realized by electron beam lithography on a Si_3N_4 -Si- Si_3N_4 sandwich, then an aperture is realized on the Si_3N_4 layer by reactive ion etching and the 400 μm thick 100-silicon substrate is removed by KOH etching. Thanks to this technique it has been possible to build the significantly long slits required for this instrument; also a line of 8 equi-spaced pinholes have been realized by the same technique, for spectrometer calibrating purposes.

Concerning the detector, to have a good coupling with the slit width, we have been looking for sensors with relatively large pixel size, of 20 μm . Unfortunately, the choice of commercial devices is rather limited, also on the basis of the relatively large size it has to have and the need to fit within the relatively small available room. Thus, at the end, we selected a smaller pixel-size detector, an active CMOS with $6480\text{H} \times 4856\text{V}$ pixels and $3.45 \times 3.45 \mu\text{m}^2$ pixel size. This sensor has a 12 bits ADC, it allows pixel binning, windowing, and read-out rates up to 12 full frames/s. The latter is an important characteristic to be able to reproduce the instrument push-broom fast acquisition mode.

The data collected by this prototype are fully representative of a flight instrument, and allow to generate the HDTM for each analyzed sample, providing the 4D information of each resolved element of the observed surface. The data reduction has been realized using an ad hoc software, derived by 3DPD (Simioni et al. (2021)), a photogrammetric pipeline developed for processing the stereo images of the Colour and Stereo Imaging System (CaSSIS) (Thomas et al. (2020)) on board of ExoMars Trace Gas Orbiter (TGO).

5. Photogrammetric activities

Any new camera system has to be properly characterized and calibrated to ensure the validity of the resulting data products. An important step in this process for the use of the stereo camera is the camera modelling. In this context, a proper stereo validation procedure has been conceived in laboratory

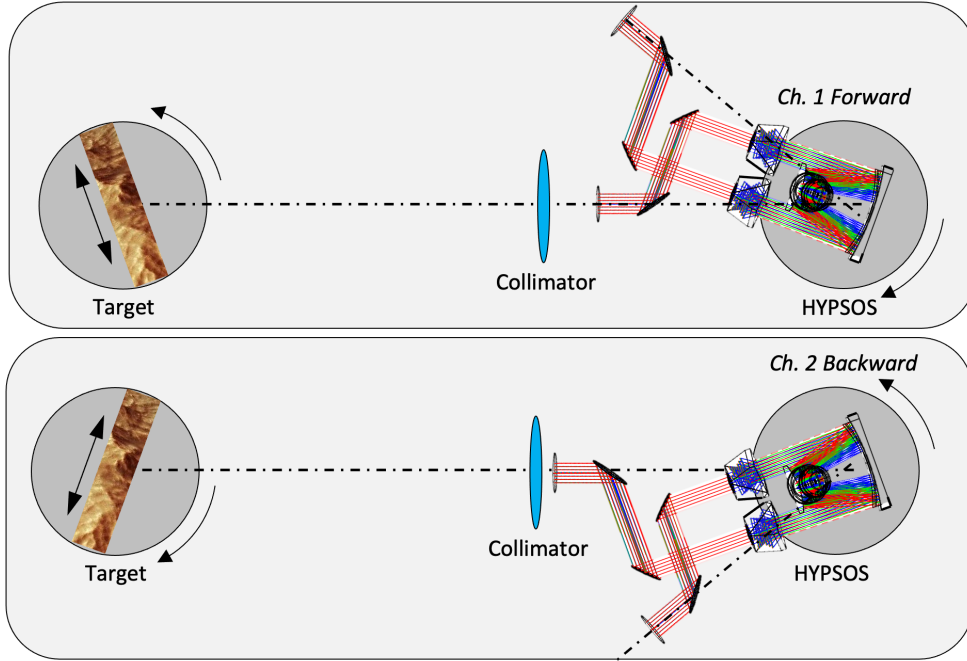


Fig. 5. HYPPOS acquisition configuration scheme. On top, the configuration for reproducing the acquisition with the forward channel is shown; on bottom, the same for the backward channel.

to demonstrate the capabilities of HYPPOS to reconstruct a 3D surface; this procedure is based on the previous experience made with STC. The described results can be used to formulate a complete methodology for stereo information extraction from a set of two images acquired with a hyperspectral pushbroom technology as HYPPOS.

To perform on the optical bench in laboratory the Stereo Validation of HYPPOS, we use a Stereo Validation Setup (SVS), which consists of the HYPPOS prototype and auxiliary optics described in the previous section, and a bi-planar calibration gauge (chessboard) of $4 \times 4 \text{ cm}^2$ shown in Figure 6 with the function of sampling source. The specifically designed reference gauge provides a high number of easily detectable reference points; based on that, the components of the projection matrix M can be estimated.

The adopted geometric calibration technique follows the method introduced by

Gupta & Hartley (1997) which, under some assumptions, allows to greatly simplify the computational steps usually involved in the push-broom model calibration. This description of a linear push-broom sensor contains the interior and exterior camera parameters with the compact representation by a projection matrix (M) that allows to apply the camera model likewise a pinhole camera model. While the pinhole model encodes a perspective projection in both horizontal and vertical (u , and v) pixel axes centered at the focal point, the push-broom model encodes a perspective transformation only along the v direction. The u direction instead encodes an orthographic projection. In the algorithm implemented in a Python code, the 3D coordinates of the bi-planar calibration gauge have been imported once accurately measured with a laser scanning system. The corresponding image coordinates, instead, have been extracted with a corner finder method of the Camera Calibration Toolbox which is included in the

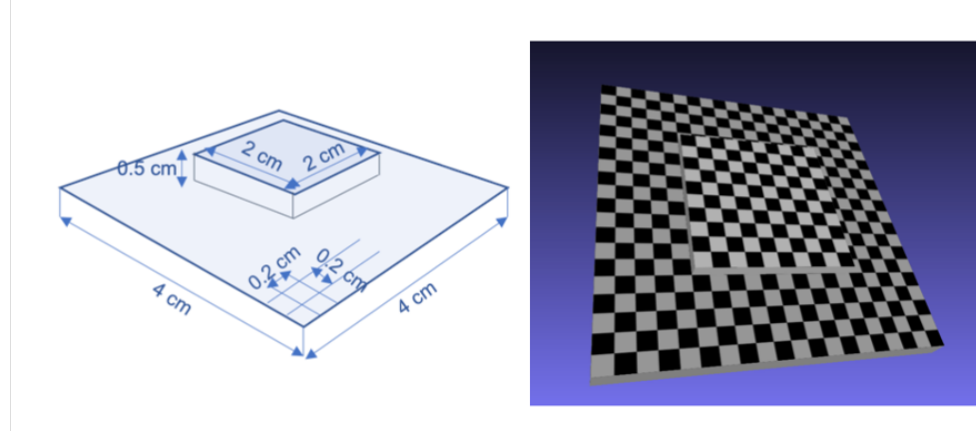


Fig. 6. On the left: Design specifications of the reference gauge, on the right: the mesh of the bi-planar gauge with a regular chessboard pattern.

OpenCV libraries from the stereo images acquired with the experimental setup. In order to model any non-linear aspects, not captured by the linear push-broom camera model, Chebyshev polynomials of the first kind T_n up to a degree of 3 have been used as the approximation functions to represent the difference between the linear camera model and the imaging characteristics of the real camera. The re-estimated camera model has been assessed by the reprojection error, where the residuals (image coordinates – projected object coordinates) $r_i = x_i - MX_i$ reach standard deviation values of less than one pixel, in particular 0.79 pixels along x and 0.95 pixels along y .

In the first phase, a set of match points (i.e., pixels in the two views that correspond to the same point in the real world, also referred to as tie points) between the two images are established by means the 3DPD software (Simioni et al. (2021)). The disparity maps refined by Least Square Matching method have been then triangulated in a second phase. With the information about the camera known by means of the gauge calibration process and defined in the correspondent projection matrices M_1 (for the image acquired with inclination of 20°) and M_2 (for the image acquired with inclination of -20°), the disparity can be analyzed to derive the 3D coordinates in the

form of a sparse point cloud or gridded DTM. In order to quantify the accuracy of the 3D reconstruction, the point cloud has been aligned with a high resolution laser scanner acquisition ($20 \mu\text{m}$ precision) used as reference. The statistics of the discrepancies between the two models are 0.136 mm in terms of standard deviation and of 0.093 mm considering the projection of the pixel on the target. The obtained results are good and lead to consider that the innovative concept of HYPPOS is able to accurately reconstruct the target surface.

6. Results

The stereo validation procedure performed in laboratory on the HYPPOS prototype permits to confirm the used methodology for obtaining a stereo hyperspectral reconstruction of the surface under observation. With the spectral and the spatial information we are able to create a representation of the surface in 3D space linked with its hyperspectral information. The quality of the spectral information depends on the adopted bandwidth, the illumination level, and the pixel position. An example of the measured HDTM is shown in Figure 7: we can see the 3D surface properties of each pixel for each spectral band, thus providing to the scientific

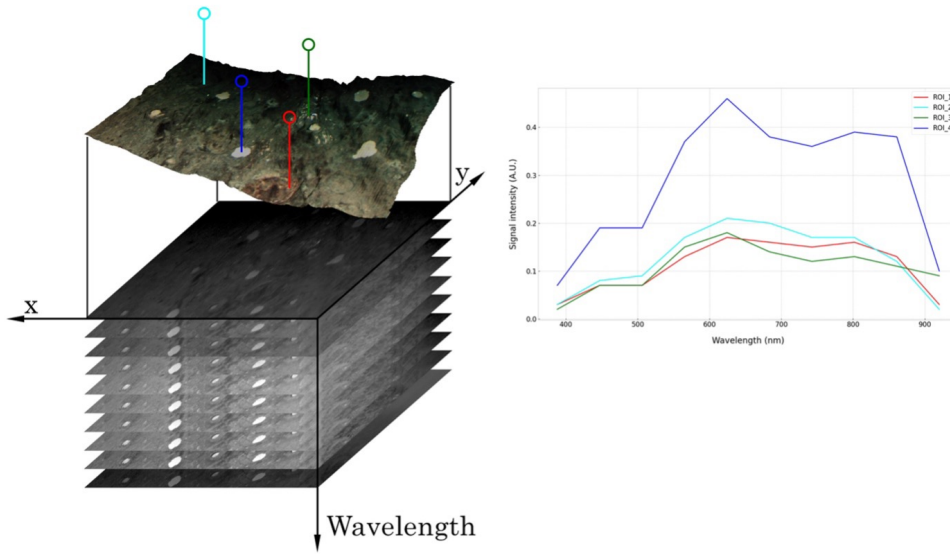


Fig. 7. HDTM: for each node of the gridded DTM, compositional information extracted from the correspondent hyperspectral images are accessible.

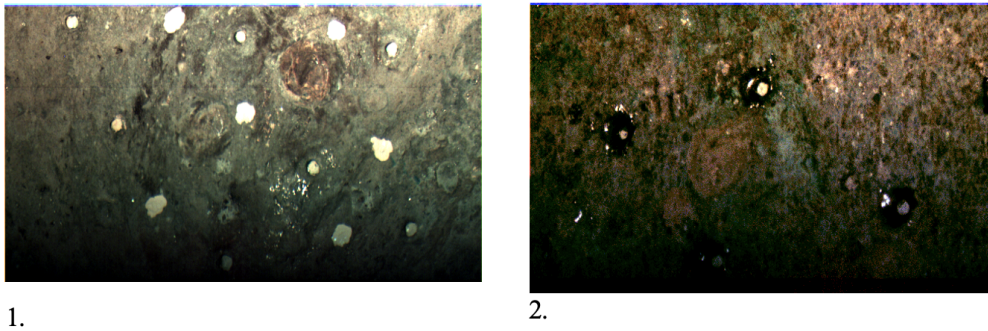


Fig. 8. 1. Near natural color combination of a reference concrete brick with added (white) targets, using 802 nm (R), 565 nm (G) and 447 nm (B) bands. 2. Composite image of an anorthosite block using 861 nm (R), 672 nm (G) and 483 nm (B) bands.

community an extremely powerful dataset for the planetary exploration.

A DTM per each spectral band has been generated showing some differences in the reconstruction due to the different ability to extract features, depending on the specific considered spectral band. We can also produce images combining different spectral bands, so highlighting different features of the surface as

a function of the observed target and of the specific investigation purposes; an example is shown in Figure 8.

7. Conclusions

We realized a prototype of the HYPerspectral Stereo Observing System in laboratory able to acquire pushbroom stereo pairs of rock samples at any spectral band allowed by the spec-

trometer. In doing so we validated the concept of a new instrument able to provide Spectral Digital Terrain Model, where at every pixel of the DTM is associated the entire spectrum. Due to the constraints on the resources in laboratory we realized the instrument working in the spectral range of 400-800 nm, but the optical design and the concept is really versatile allowing to implement a second channel working in the infrared and the camera, the first half of the instrument, may have a longer focal length providing a better spatial resolution.

HYPPOS is the merging of a stereo camera with a spectrometer and the illumination conditions are the same. If we assume a satellite with the two separate instruments, the stereo camera would have the lines of sight as expected for HYPPOS while the spectrometer would be nadir pointing, it means the difference in the phase angle would be only of 15-20 degrees.

In the case of HYPPOS there is not this difference and there would be a slightly lower SNR only for the spectrometer section, with respect to the two separate instruments.

The fact to have the opportunity to exploit both in one shot and the importance to exploit a highly innovative data fused digital product as the hyperspectral 3D, highly overcome an issue concerning the optimal observation condition.

The goal of the project, funded by ASI, was to demonstrate that is possible to provide with a single instrument the 3D and spectral information of any feature on a planetary surface and the it has been achieved.

Authors

P. Palumbo⁵, M. Pertile⁴, A. Petrella¹, G. Salemi⁸, A.C. Tangari⁷, M. Zusi⁵

Affiliations

⁶ CNR - Institute of Photonics and Nanotechnologies, Roma, via Cineto Romano, 42, 00156 Roma, Italy

⁷ Department of Psychological Sciences, Health and Territory, University "G. D'annunzio" Chieti-Pescara, Via dei Vestini - campus universitario, 66100 Chieti, Italy

⁸ Department of Cultural Heritage, University of Padova, Piazza Capitaniato 7, 35139, Padova, Italy

Acknowledgements. This project has been realized thanks to the contributions of the Italian Space Agency (ASI) and the Italian National Institute of AstroPhysics (INAF) under the ASI-INAF agreement 2018-16.HH.0.

References

- Cremonese, G., et al., 2020, Space Sci. Rev., 216, 75
- Da Deppo, V., et al., 2010, Appl. Opt., 49, 2910
- Grotzinger, J., Milliken, R., 2012. The Sedimentary Rock Record of Mars: Distribution, Origins, and Global Stratigraphy. SEPM Special Publication No. 102: Sedimentary Geology of Mars. 102, 1
- Gupta, R., & Hartley, R.I., 1997, IEEE Trans. Pattern Anal. Mach. Intell. 19 (9), 963
- Mattioli, F., et al., 2011, Microelectron. Eng. 88(8), 2330
- Naletto, G., et al., 2012, SPIE Proc. 8442, Article Number 84421M
- Naletto, G., et al., 2023, SPIE Proc. 12777, Article Number 127775C
- Rispoli, R., et al., 2013, Optical Engineering 52(5), 051206
- Simioni, E., et al., 2017, ICSO 2014, SPIE Proc. 10563, Article number 105634E
- Simioni, E., et al., 2021, Planet. Space Sci., 198, 105165
- Thomas, N., et al., 2020, Space Sci. Rev., 212, 1897
- Tordi, M., et al., 2020, Optical, Infrared, and Millimeter Wave, Proc. SPIE11443, Article number 114437C